AJNR

Differentiation between Brain Glioblastoma Multiforme and Solitary Metastasis: Qualitative and Quantitative Analysis Based on Routine MR Imaging

X.Z. Chen, X.M. Yin, L. Ai, Q. Chen, S.W. Li and J.P. Dai

AJNR Am J Neuroradiol 2012, 33 (10) 1907-1912
doi: https://doi.org/10.3174/ajnr.A3106
http://www.ajnr.org/content/33/10/1907

ORIGINAL RESEARCH

Differentiation between Brain Glioblastoma Multiforme and Solitary Metastasis: Qualitative and Quantitative Analysis Based on Routine MR Imaging

X.Z. Chen
X.M. Yin
L. Ai
Q. Chen
S.W. Li
J.P. Dai

EDITOR'S CHOICES

BACKGROUND AND PURPOSE: The differentiation between cerebral GBM and solitary MET is clinically important and may be radiologically challenging. Our hypothesis is that routine MR imaging with qualitative and quantitative analysis is helpful for this differentiation.

MATERIALS AND METHODS: Forty-five GBM and 21 solitary metastases were retrospectively identified, with their preoperative routine MR imaging analyzed. According to the comparison of the area of peritumoral T2 prolongation with that of the lesion, the tumors were classified into grade I (prolongation area ≤ tumor area) and grade II (prolongation area > tumor area). The signal intensities of peritumoral T2 prolongation were measured on T2WI and normalized to the values of the contralateral normal regions by calculating the ratios. The ratio (nSI) of both types of tumors was compared in grade I, grade II, and in tumors without grading. The best cutoff values to optimize the sensitivity and specificity were determined for optimal differentiation.

RESULTS: The nSI of GBM was significantly higher than that of MET without T2 prolongation grading ($P < .001$), resulting in AUC = 0.725. The difference was significant ($P = .014$) in grade I tumors (GBM, 38; MET, 9), with AUC = 0.741, and in grade II tumors (GBM, 7; MET, 12), with AUC = 0.869 ($P = .017$). Both types of tumors showed a different propensity in T2 prolongation grading ($\chi^2 = 12.079$, $P = .001$).

CONCLUSIONS: Combined with qualitative and quantitative analysis of peritumoral T2 prolongation, routine MR imaging can help in the differentiation between brain GBM and solitary MET.

ABBREVIATIONS: AUC = area under the ROC curve; GBM = glioblastoma multiforme; MET = metastasis; nSI = normalized signal intensity; ROC = receiver operating characteristic; WHO = World Health Organization

BRAIN

ORIGINAL RESEARCH

Differentiation between cerebral solitary MET and GBM is very important because of their vast differences in clinical staging, surgical planning, and therapeutic decisions.[1] On routine MR imaging scans (precontrast T1WI and T2WI and postcontrast images), the 2 types of tumors usually demonstrate similar radiologic appearance: an obviously necrotic mass, with strong peritumoral T2 prolongation on unenhanced images, and ringlike enhancement on postcontrast images.[2,3] Therefore, it is thought to be very difficult to distinguish between these 2 types of tumors with routine MR imaging alone.[4-6] Many studies have focused on other advanced MR imaging modalities, such as DTI,[3,5,7,8] DWI,[9,10] PWI,[6,11-16] and MR spectroscopy,[17] to explore the differentiating characteristics.

In DTI studies, the metrics of mean diffusivity, fractional anisotropy, linear anisotropy coefficients, and planar anisotropy coefficients showed significant differences between the 2 types of tumors.[3,5,8] DWI research demonstrated that the mean minimum ADC values and mean ADC ratios in the peritumoral regions of GBM were significantly higher than those in MET.[10] With PWI, most of the studies showed that the CBV of GBM was significantly higher than in MET, either in the peritumoral region[11-13] or in the enhanced region.[14] An MR spectroscopy study indicated that lipid and macromolecule signals were significantly different between the 2 types of tumors.[17]

Overall, all of the advanced MR imaging modalities used semiquantitative or quantitative analysis for this differentiation, while routine MR imaging is commonly based on morphologic appearance alone. Thus, our hypothesis is that routine MR imaging with qualitative and quantitative analysis is helpful for this differentiation.

Materials and Methods

Written informed consent was waived, and the institutional review committee approved this study.

Patients

The MR imaging examinations of 66 consecutive patients (43 men, 23 women; age range 21–74 years; mean age 51.6 ± 11.6 years) with a

Received January 3, 2012; accepted after revision February 14.

From the Department of Neuroimaging (X.Z.C., L.A., S.W.L., J.P.D.), Beijing Tiantan Hospital, Capital Medical University, Beijing, P. R. China; Radiology Department (X.M.Y.), China Coal General Hospital, Beijing; Department of Neuroimaging (Q.C.), Beijing Neurosurgical Institute Hospital, Capital Medical University, Beijing.

C.X. and Y.X. contributed equally to this study.

This study is supported by the funding of Natural Science Foundation of China (Grant numbers: 81071139, 81071137, and 30770617) and training program of Beijing Health System high-level health and technical personnel (Grant number: 2011-3-0377).

Please address correspondence to Dai Jianping, MD, Department of Neuroimaging, Beijing Tiantan Hospital, Capital Medical University, Beijing, P. R. China, Address: No. 6 Tiantan Xili, Chongwen District, Beijing, P. R. China, Postcode: 100050; e-mail: djpbeijing@hotmail.com

http://dx.doi.org/10.3174/ajnr.A3106

Table 1: nSI from 2 radiologists

Tumor	1st Measurement	2nd Measurement	Pearson Correlative Analysis
GBM	3.1 ± 0.48	3.15 ± 0.5	$P < .001$, $r = .894$
MET	2.73 ± 0.3	2.74 ± 0.35	$P < .001$, $r = .918$
Total	2.98 ± 0.46	3.02 ± 0.45	$P < .001$, $r = .912$

diagnosis of GBM or solitary MET were evaluated retrospectively. All patients had a previously untreated solitary enhancing brain tumor and peritumoral T2 prolonged signals, and had undergone routine brain MR examination before surgical resection at our institution between May 2009 and November 2010. Their tumors fulfilled the 2007 WHO histopathologic criteria for the diagnosis.[18] Patients with hemorrhagic tumors were not included in the study because intratumoral hemorrhage may affect peritumoral T2 prolonged signals. Tumors with minimal peritumoral T2 prolongation (area <1/4 tumor area on the axial section where the tumor showed maximal diameter) were excluded.

The final diagnosis was based on intraoperative observations and histopathologic findings. Of the 66 patients, WHO grade IV GBM was diagnosed in 45 cases (30 men, 15 women; mean age 50.5 ± 12.4 years; range 21–72 years) and solitary MET was diagnosed in 21 cases (13 men, 8 women; mean age 54 ± 9.6 years; range 36–74 years). Metastatic brain tumors included carcinomas from lung ($n = 10$), thyroid ($n = 1$), ovary ($n = 1$), rectum ($n = 1$), endometrium ($n = 1$), and unknown origin ($n = 7$).

MR Imaging and Processing

All MR imaging examinations were performed within 7 days before surgery. The protocol included unenhanced and enhanced sequences. The precontrast sequence consisted of axial T1WI, T2WI, and sagittal T1WI. Once the precontrast imaging was completed, 0.2 mL/kg gadopentetate dimeglumine (Magnevist; BayerHealthCare Pharmaceuticals, Wayne, New Jersey) was administered manually via the antecubital vein by a registered nurse. Postcontrast images, including the axial, sagittal, and coronal images, were obtained immediately after the administration of contrast media. Thirty patients were scanned on a Genesis Signa 3T scanner (GE Healthcare, Milwaukee, Wisconsin). A T1-weighted sequence (TR/TE, 2031/19) and FSE T2WI (TR/TE, 4900/117) were performed with the same field of view (240 mm) and matrix (512 × 512). Thirty-six patients underwent MR imaging on another 3T superconducting MR scanner (Magnetom, Trio; Siemens, Erlangen, Germany). A T1-weighted turbo inversion recovery sequence (TR/TE, 2000/9.8) and T2-weighted turbo spin-echo scan (TR/TE, 4500/84) were obtained. The section thickness and gap were 5 mm and 6 mm, respectively, regardless of the scanner used.

Peritumoral T2 prolongation was defined as an area clearly outside the well-defined enhancing solid portion of the tumor that contained absolutely no enhancement and showed high signal intensity on T2WI. For internal control, normal-appearing mirrored regions were located on the contralateral hemisphere that contained no enhancement and showed normal signal intensity on T2WI.

To determine the peritumoral signal intensity, ROIs were placed in the regions of peritumoral T2 prolongation surrounding each tumor using the software Neusoft PACS (downloaded from http://www.neusoft.com). For each ROI in the peritumoral T2 prolongation, a mirror ROI was placed in the same anatomic region on the contralateral normal-appearing hemisphere. The placement of the mirror ROI avoided areas of necrotic tissue, cysts, and large vessels, as much as possible.

After placement of each ROI, the signal intensity on T2WI was automatically measured by the software. First, we selected all continuous sections that included the peritumoral T2 prolongation. To account for the heterogeneity of the prolongation, 4 uniformly round or ovoid ROIs (area 10–12 mm^2) were carefully placed in different regions of the peritumoral T2 prolongation by visual inspection. To avoid a transverse partial volume effect, the locations of ROIs were 3–4 mm away from the outer margins of the prolongation and the enhancing margin of the tumor, with reference to the same section on enhanced T1WI. To avoid longitudinal partial volume averaging, the chosen sections were covered by at least 1 section with T2 prolongation inferiorly and superiorly.

For each peritumoral ROI and its mirror counterpart, the nSI was calculated by dividing the signal intensity value of the ROI on the affected hemisphere by that of the mirror ROI on the contralateral hemisphere, similar to the previously published method.[11] For each tumor, the nSI was defined as the mean ratio of the 4 pairs of ROIs and mirror ROIs. These measurements and calculations were performed independently by 2 experienced radiologists. The averaged nSI from the 2 observers was considered as the final nSI for the statistical analysis.

A subjective grading system for the peritumoral T2 prolongation, similar to what has been reported,[19] was used—for grade I, the area of peritumoral T2 prolongation ≤ the area of the tumor on the section where the tumor showed maximal diameter; for grade II, the area of peritumoral T2 prolongation > the area of the enhancing tumor.

The ROI positioning, nSI calculation, and T2 grading were conducted by 2 radiologists (Q.C., 16 years of experience, and S.W.L., 16 years of experience) independently. They were blinded to each other and to the clinical and pathologic information. Discrepancies of T2 prolongation grading were resolved by consensus.

Statistical Analysis

A 1-sample Kolmogorov-Smirnow test was used to determine whether the data were in normal distribution. To compare the differences between the patient age, sex, and the nSI in different T2 prolongation grading, a χ^2 test or a t test was used. The nSIs produced by the 2 MR scanners were also compared with the t test to determine whether the measurement was affected by MR scanners. Correlative analysis was used to test the consistency of the 2 individual measurements made by the 2 radiologists. ROC analysis was applied to assess the best cutoff value of the nSI that had the optimal combination of the sensitivity and specificity in distinguishing between GBM and solitary MET. A χ^2 test was also used to test the difference of T2 prolongation grading between the 2 types of tumors.

Statistical analysis was performed on commercial statistical software (Statistical Package for the Social Sciences, Version 13.0; SPSS, Chicago, Illinois). P values < .05 were considered statistically significant.

Results

The data of patient age and nSI were in normal distribution. No difference between GBM and solitary MET in patient sex

Table 2: Final nSI of patients scanned by different MR scanners

Tumor	Genesis Signa (n)	Magnetom Trio (n)	*P* Value
GBM	3.16 ± 0.48 (19)	3.1 ± 0.49 (26)	.676
MET	2.85 ± 0.35 (11)	2.61 ± 0.25 (10)	.098
Total	3.05 ± 0.46 (30)	2.97 ± 0.48 (36)	.484

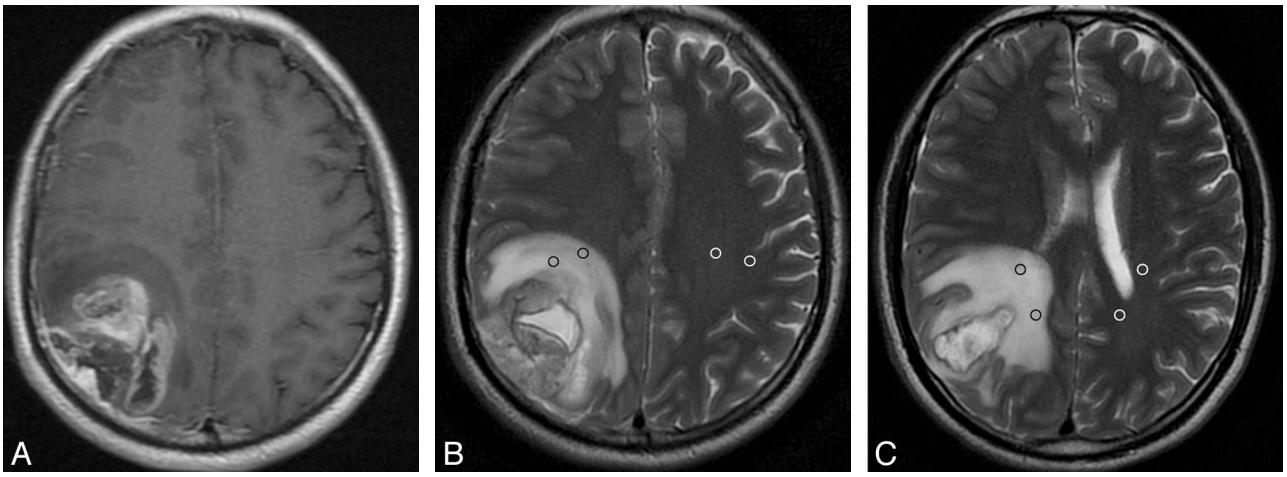

Fig 1. GBM with peritumoral T2 prolongation of grade I. Postcontrast axial T1WI shows a heterogeneously enhancing lesion in the right parietal lobe with a maximal diameter of 4.5 cm (*A*). On the same section as *A*, axial T2WI demonstrates medium peritumoral T2 prolongation, which is smaller in area than the tumor (*B*). Two ROIs are placed in the prolonged region (*black ring*), with 2 mirror ROIs in the contralateral region (*white ring*). On the section inferior to *B*, another 2 ROIs are positioned in the hyperintense region and, accordingly, 2 mirror ROIs are placed in the contralateral region (*C*). For this measurement, the mean value of signal intensity is 852.5 for the prolonged region and 231.5 for the intact contralateral region. Thus, the nSI is 3.68 (852.5/231.5).

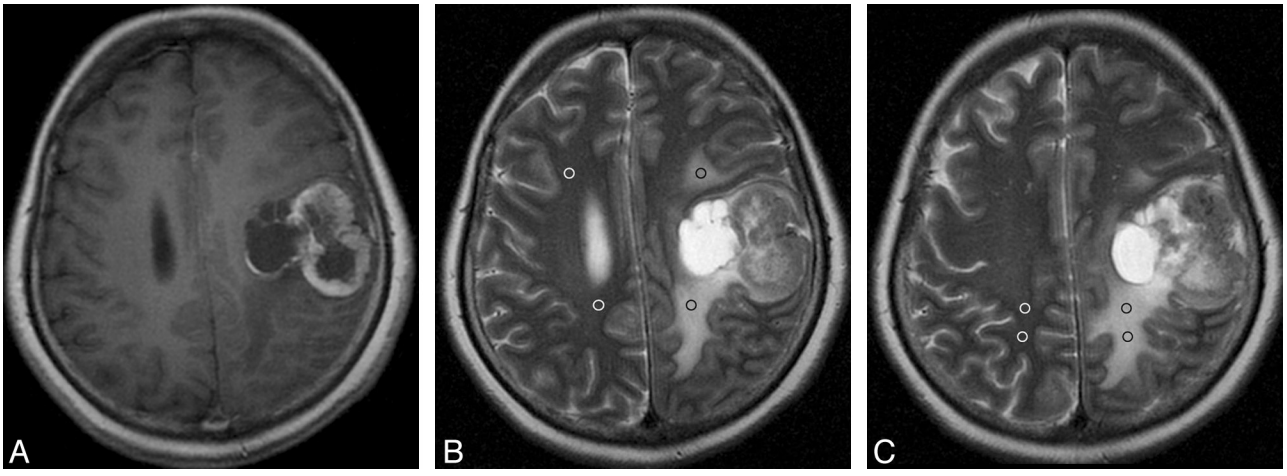

Fig 2. Solitary MET with peritumoral T2 prolongation of grade I. Postcontrast axial T1WI shows a heterogeneously enhancing lesion in the left frontal and anterior parietal lobes with a maximal diameter of 3.94 cm (*A*). On the same section as *A*, axial T2WI demonstrates medium peritumoral T2 prolongation, which is smaller in area than the tumor (*B*). On this section, 2 ROIs are placed in the prolonged region (*black ring*), with 2 mirror ROIs in the contralateral area (*white ring*). On the section superior to *B*, another 2 ROIs with 2 mirror ROIs are positioned in the prolongation region and the contralateral region, respectively (*C*). For this measurement, the mean value of signal intensity is 818.0 for the prolonged region and 280.5 for the intact contralateral region, respectively. Thus, the nSI is 2.92 (818.0/280.5).

($\chi^2 = 0.175$, $P = .676$), or patient age ($P = .281$) was found. There was high consistency between the 2 separate measurements from the 2 radiologists (Table 1). The peritumoral signal intensity was not influenced by different MR scanners (Table 2). With regard to the grading of peritumoral T2 prolongation, 47 cases were grade I (GBM, 38; MET, 9; Figs 1 and 2) and 19 cases were grade II (GBM, 7; MET, 12; Figs 3 and 4), showing a significant difference between GBM and MET ($\chi^2 = 12.079$, $P = .001$). In addition, the final nSI of GBM was significantly higher than that of MET in grade I ($P = .014$) and grade II ($P = .017$), as well as both combined ($P < .001$; Fig 5). ROC analysis showed a larger AUC among grade II tumors (Table 3).

Discussion

In our study, qualitative analysis showed that GBM was more likely to have a grade I pattern and single MET was more likely to have a grade II pattern ($\chi^2 = 12.079$, $P = .001$); quantitative analysis indicated that the nSI of GBM was significantly higher than that of MET ($P < .001$). Furthermore, ROC analysis demonstrated that the AUC increased from 0.741 to 0.869 as the peritumoral T2 prolongation aggravated from grade I to grade II, indicating that the larger the area of peritumoral T2 prolongation is, the more significant the difference in nSI is. This may be explained by different mechanisms of peritumoral T2 prolongation.

Generally speaking, the peritumoral T2 prolongation of the 2 types of tumors is vasogenic[3]; however, the detailed mechanism is different. In MET, no histologic evidence of tumors has been found in the peritumoral region of T2 prolongation.[20,21] The white matter fiber tracts in such regions are compressed and shifted.[5] These regions are intrinsically normal brain parenchyma, with purely vasogenic edema caused by the disruption of the blood-brain barrier and increased interstitial water contents from leaky capillaries.[22,23] Gliomas, however, are well known for their characteristic infiltration through

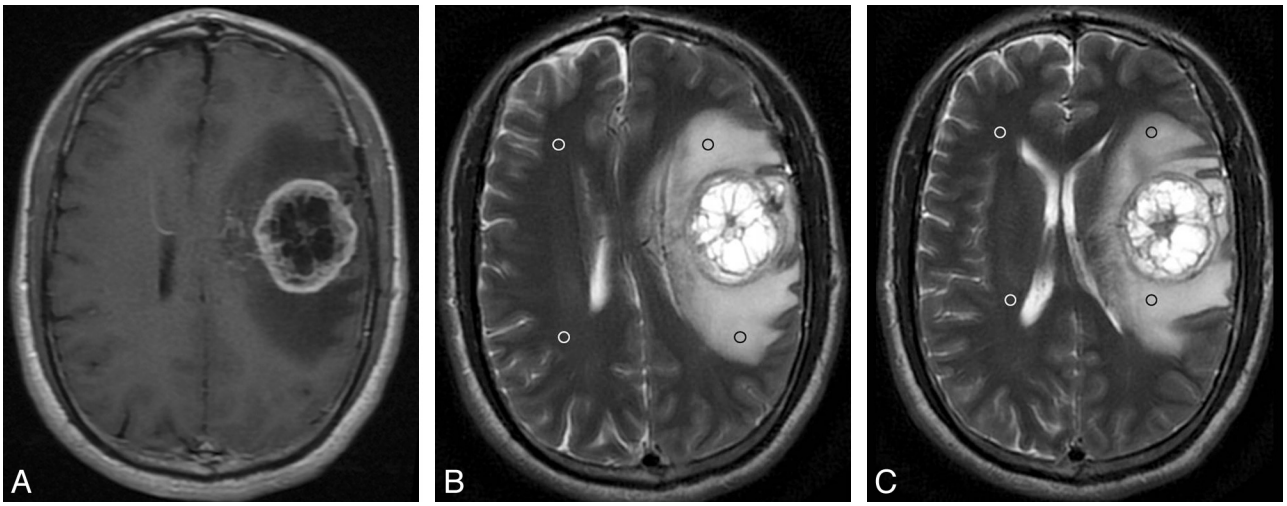

Fig 3. GBM with peritumoral T2 prolongation of grade II. Postcontrast axial T1WI reveals a ringlike enhancing lesion in the left frontal lobe with a maximal diameter of 4.05 cm (*A*). On the same section as *A*, axial T2WI demonstrates obvious peritumoral hyperintensity, which is larger in area than the tumor (*B*). Two ROIs are placed in the prolonged region (*black ring*), with 2 mirror ROIs in the contralateral side (*white ring*). On the section inferior to *B*, 2 additional ROIs are positioned in the prolonged region and, accordingly, 2 mirror ROIs are placed in the contralateral side (*C*). The nSI is 4.18 (692.5/165.5).

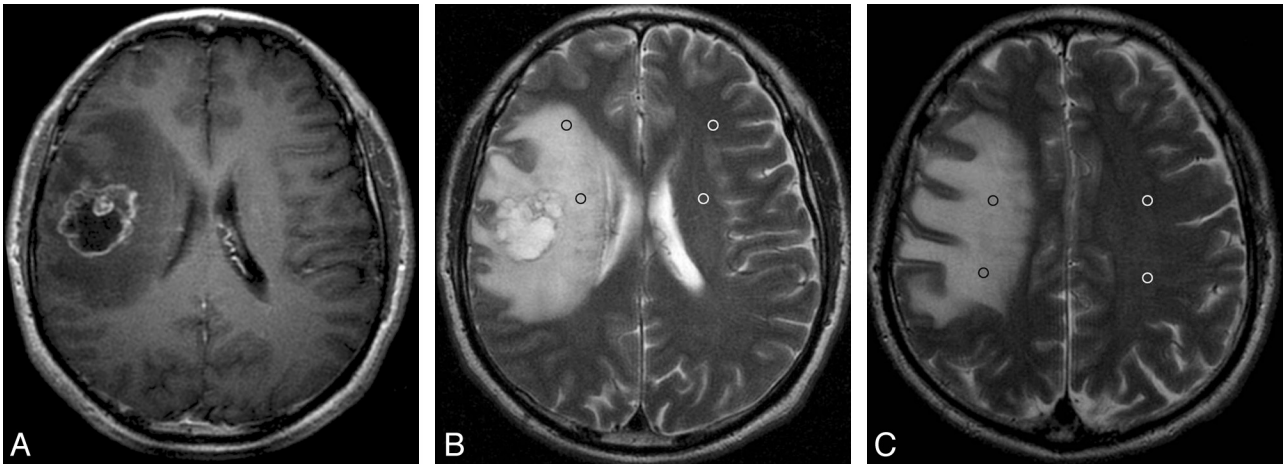

Fig 4. Solitary MET with peritumoral T2 prolongation of grade II. Postcontrast axial T1WI shows a ringlike enhancing lesion in the right frontal lobe with a maximal diameter of 3.6 cm (*A*). On the same section as *A*, axial T2WI demonstrates strong peritumoral T2 prolongation, which is larger in area than the tumor (*B*). On this section, 2 ROIs and 2 mirror ROIs are placed in the prolonged region (*black ring*) and contralateral area (*white ring*). On the section superior to *A*, another 2 ROIs with 2 mirror ROIs are positioned in the prolonged region and the contralateral region, respectively (*C*). The nSI is 2.75 (603.5/219.5).

white matter fiber tracts.[24,25] Pathologically, GBM has 3 types of infiltration: infiltration with single cells, with cell nests, and with demarcation of a relatively sharp border.[26] Histologically, neoplastic cells have been found in the T2 prolonged regions surrounding GBM.[12,27] Therefore, the peritumoral T2 prolongation of GBM is caused by a combination of vasogenic edema and tumoral infiltration simultaneously.[28] Further research demonstrated that the perifocal T2 prolongation of GBM not only includes invading tumor cells but also is associated with glial alterations in vital brain tissue.[29] These differences in the mechanism of peritumoral T2 prolongation formation may explain our finding that the peritumoral nSI of GBM is higher than that of MET.

Many articles have been published comparing the differences between GBM and solitary MET via different imaging modalities. According to the anatomic location being researched, these can be divided into 3 types. The first type is focused on 2 anatomic locations: the enhancing portions of the tumor and the peritumoral regions with T2 prolongation.[3,5,6,8-10,13,15] The second mainly deals with 1 location: either the enhancing part of the tumor[14,16,17] or the surrounding hyperintense region on the T2WI.[11,12] The third type is focused on 3 locations: the enhancing part of the tumor, regions with peritumoral T2 prolongation, and the necrotic areas within the tumor.[7] With regard to the enhancing part of the tumor, DTI and perfusion metrics showed inconsistent conclusions, with some authors believing there was no difference between the 2 types of tumors,[10,13,16] contrary to the others.[6,8,14,15] As for the peritumoral T2 prolongation, the results were also controversial. Some articles demonstrated that the region was helpful in the differentiation between GBM and MET by DWI, DTI, and PWI metrics,[6,8,10,13,15] which is inconsistent with other papers.[5,7] In some research, the peritumoral T2 prolonged region was artificially divided into 2 parts: the proximal edema and the distal edema, and the results indicated that the proximal edema was helpful for the differentiation.[8,9,11] In our opinion, to some extent, the discrepancies may be related to the bias of section selection and ROI positioning.

In this study, we focused only on the peritumoral T2 pro-

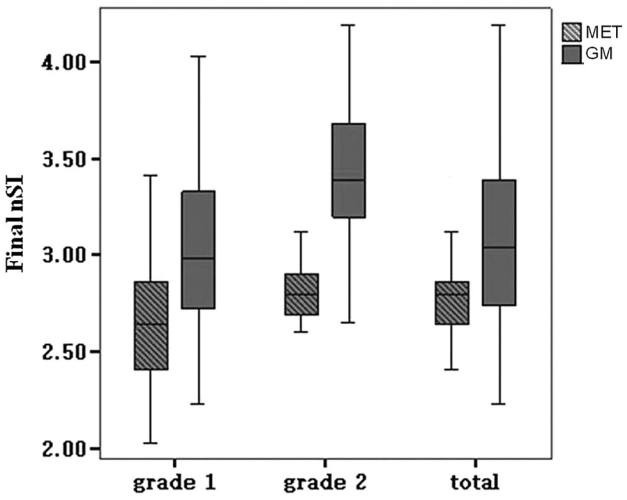

Fig 5. Box-and-whisker plots. Thick horizontal line = mean; whiskers = ± SD. The final nSI of peritumoral T2 in GBM is significantly higher than that of solitary MET in grade I ($P = .014$), grade II ($P = .017$), and tumors as a whole without grading ($P < .001$).

Table 3: Sensitivity and specificity of final nSI of peritumoral T2 prolongation with high predictive power in differentiating GBM from solitary MET using ROC analysis

Peritumoral T2 Prolongation Grading	Cutoff Value	Sensitivity	Specificity	AUC
Grade I	2.44	0.974	0.444	0.741
Grade II	3.085	0.857	0.917	0.869
Total	2.88	0.644	0.762	0.725

longation and took it as a whole, without artificial division. The largest AUC of 0.869 is smaller than the previously reported observations (0.938[8] and 0.98[13]). Considering that this is from a routine MR examination, an imaging technique that is the least time-consuming and the most practical in different medical institutes, and a ROI positioning method that is least restrictive, we believe that the results of our study are acceptable and bear practical significance.

Our study has some limitations. As a retrospective study, it may have a selective bias inherent to clinical case series. Another limitation is the use of 2 different MR scanners with different parameters. This may influence the measurement of signal intensity to some extent. However, statistical analysis of data from the different scanners and imaging parameters did not support this speculation, indicating that our method may be universally useful. The third limitation is that the peritumoral T2 prolongation grading is not completely accurate. It would be more accurate if we had measured the volumes of the peritumoral T2 prolongation and tumor with automation by using software programs. We think, however, this grading system from volume calculation is bound to be a time-consuming procedure and may limit wide application in clinical settings. Finally, the number of cases with solitary MET may be too small to compare the peritumoral T2 prolongation of MET from different origins.

Conclusions

Combined with qualitative and quantitative analysis of peritumoral T2 prolongation, routine MR imaging can be helpful in distinguishing GBM from brain solitary MET. Given its availability and simplicity, we believe this method has practical significance.

Acknowledgments

We thank Xiaojuan Ru, MD, Department of Neuroepidemiology, Beijing Neurosurgical Institute for her statistical analysis. We also thank Yihua Zhou, MD, PhD, Neuroradiology Division, Department of Radiology, University of Pittsburgh Medical Center, Pittsburgh, Pennsylvania, for his English editing.

Disclosures: Ai Lin—*RELATED: Grant:* National Natural Science Foundation of China (30770617, 81071139),* Beijing Sci-Tech Nova Plan B (2007B052).* (* *Money paid to institution*)

References

1. Campos S, Davey P, Hird A, et al. **Brain metastasis from an unknown primary, or primary brain tumour? A diagnostic dilemma.** *Curr Oncol* 2009;16:62–66
2. Schwartz KM, Erickson BJ, Lucchinetti C. **Pattern of T2 hypointensity associated with ring-enhancing brain lesions can help to differentiate pathology.** *Neuroradiology* 2006;48:143–49
3. Byrnes TJ, Barrick TR, Bell BA, et al. **Diffusion tensor imaging discriminates between glioblastoma and cerebral metastases in vivo.** *NMR Biomed* 2011;24:54–60
4. Cha S, Knopp EA, Johnson G, et al. **Intracranial mass lesions: dynamic contrast-enhanced susceptibility-weighted echo-planar perfusion MR imaging.** *Radiology* 2002;223:11–29
5. Tsuchiya K, Fujikawa A, Nakajima M, et al. **Differentiation between solitary brain metastasis and high-grade glioma by diffusion tensor imaging.** *Br J Radiol* 2005;78:533–37
6. Cha S, Lupo JM, Chen MH, et al. **Differentiation of glioblastoma multiforme and single brain metastasis by peak height and percentage of signal intensity recovery derived from dynamic susceptibility-weighted contrast-enhanced perfusion MR imaging.** *AJNR Am J Neuroradiol* 2007;28:1078–84
7. Toh CH, Wei KC, Ng SH, et al. **Differentiation of brain abscesses from necrotic glioblastomas and cystic metastatic brain tumors with diffusion tensor imaging.** *AJNR Am J Neuroradiol* 2011;32:1646–51
8. Wang S, Kim S, Chawla S, et al. **Differentiation between glioblastomas, solitary brain metastases, and primary cerebral lymphomas using diffusion tensor and dynamic susceptibility contrast-enhanced MR imaging.** *AJNR Am J Neuroradiol* 2011;32:507–14
9. Oh J, Cha S, Aiken AH, et al. **Quantitative apparent diffusion coefficients and T2 relaxation times in characterizing contrast enhancing brain tumors and regions of peritumoral edema.** *J Magn Reson Imaging* 2005;21:701–08
10. Lee EJ, terBrugge K, Mikulis D, et al. **Diagnostic value of peritumoral minimum apparent diffusion coefficient for differentiation of glioblastoma multiforme from solitary metastatic lesions.** *AJR Am J Roentgenol* 2011;196:71–76
11. Lehmann P, Saliou G, de Marco G, et al. **Cerebral peritumoral oedema study: does a single dynamic MR sequence assessing perfusion and permeability can help to differentiate glioblastoma from metastasis?** *Eur J Radiol* 2012;81:522–27
12. Blasel S, Jurcoane A, Franz K, et al. **Elevated peritumoural rCBV values as a mean to differentiate metastases from high-grade gliomas.** *Acta Neurochir (Wien)* 2010;152:1893–99
13. Server A, Orheim TE, Graff BA, et al. **Diagnostic examination performance by using microvascular leakage, cerebral blood volume, and blood flow derived from 3-T dynamic susceptibility-weighted contrast-enhanced perfusion MR imaging in the differentiation of glioblastoma multiforme and brain metastasis.** *Neuroradiology* 2011;53:319–30
14. Young GS, Setayesh K. **Spin-echo echo-planar perfusion MR imaging in the differential diagnosis of solitary enhancing brain lesions: distinguishing solitary metastases from primary glioma.** *AJNR Am J Neuroradiol* 2009;30:575–77
15. Ma JH, Kim HS, Rim NJ, et al. **Differentiation among glioblastoma multiforme, solitary metastatic tumor, and lymphoma using whole-tumor histogram analysis of the normalized cerebral blood volume in enhancing and perienhancing lesions.** *AJNR Am J Neuroradiol* 2010;31:1699–706
16. Calli C, Kitis O, Yunten N, et al. **Perfusion and diffusion MR imaging in enhancing malignant cerebral tumors.** *Eur J Radiol* 2006;58:394–403
17. Opstad KS, Murphy MM, Wilkins PR, et al. **Differentiation of metastases from high-grade gliomas using short echo time ^{1}H spectroscopy.** *J Magn Reson Imaging* 2004;20:187–92
18. Rousseau A, Mokhtari K, Duyckaerts C. **The 2007 WHO classification of tumors of the central nervous system–what has changed?** *Curr Opin Neurol* 2008;21:720–27
19. Pereira-Filho Nde A, Soares FP, Chemale Ide M, et al. **Peritumoral brain edema in intracranial meningiomas**. *Arq Neuropsiquiatr* 2010;68:346–49

20. Mechtler L. **Neuroimaging in neuro-oncology.** *Neurotherapeutics* 2009;27:171–201
21. Cha S. **Perfusion MR imaging of brain tumors.** *Top Magn Reson Imaging* 2004; 15:279–89
22. Machein MR, Plate KH. **VEGF in brain tumors.** *J Neurooncol* 2000;50:109–20
23. Strugar J, Rothbart D, Harrington W, et al. **Vascular permeability factor in brain metastases: correlation with vasogenic brain edema and tumor angiogenesis.** *J Neurosurg* 1994;81:560–66
24. Chen X, Dai J, Jiang T. **Supratentorial WHO grade II glioma invasion: a morphologic study using sequential conventional MRI.** *Br J Neurosurg* 2010;24: 196–201
25. Chen XZ, Jiang T, Li SW, et al. **Dynamic radiological change of gliomas located in the paralimbic system and its clinical significance.** *Chin Med J (Engl)* 2008; 121:713–15
26. Duenisch P, Reichart R, Mueller U, et al. **Neural cell adhesion molecule isoform 140 declines with rise of WHO grade in human gliomas and serves as indicator for the invasion zone of multiform glioblastomas and brain metastases.** *J Cancer Res Clin Oncol* 2011;137:399–414
27. Kelly PJ, Daumas-Duport C, Scheithauer BE, et al. **Stereotactic histologic correlations of computed tomography and magnetic resonance imaging defined abnormalities in patients with glial neoplasms.** *Mayo Clin Proc* 1987;62: 450–59
28. Stummer W. **Mechanisms of tumor-related brain edema.** *Neurosurg Focus* 2007;15:E8
29. Engelhorn T, Savaskan NE, Schwarz MA, et al. **Cellular characterization of the peritumoral edema zone in malignant brain tumors.** *Cancer Sci* 2009;100: 1856–62